JHR 87: 223–233 (2021)
doi: 10.3897/jhr.87.67256
https://jhr.pensoft.net

RESEARCH ARTICLE

JOURNAL OF Hymenoptera RESEARCH
A peer-reviewed open-access journal
The International Society of Hymenopterists

Janzenella theia Bremer & Talamas (Platygastroidea, Janzenellidae): a new species from Baltic amber

Jonathan Bremer[1], Thomas van de Kamp[2], Elijah J. Talamas[1]

1 *Florida State Collection of Arthropods, Division of Plant Industry, Florida Department of Agriculture and Consumer Services, Gainesville, FL, USA* **2** *Karlsruhe Institute of Technology, Karlsruhe, Germany*

Corresponding author: Elijah J. Talamas (elijah.talamas@fdacs.gov)

Academic editor: Zachary Lahey | Received 12 April 2021 | Accepted 20 May 2021 | Published 23 December 2021

http://zoobank.org/FB31C313-3609-43B8-AB6A-9698FE22ACDB

Citation: Bremer J, Kamp T, Talamas EJ (2021) *Janzenella theia* Bremer & Talamas (Platygastroidea, Janzenellidae): a new species from Baltic amber. In: Lahey Z, Talamas E (Eds) Advances in the Systematics of Platygastroidea III. Journal of Hymenoptera Research 87: 223–233. https://doi.org/10.3897/jhr.87.67256

Abstract

A new species, *Janzenella theia* Bremer & Talamas, **sp. nov.**, is described from Baltic amber, which is the second known species of the family Janzenellidae (Platygastroidea). Synchrotron scanning was performed to observe internal structures and external morphology that was occluded by turbidity in the amber matrix surrounding the specimen.

Keywords

Eocene, paleontology, synchrotron

Introduction

Platygastroid wasps are well represented in amber deposits, offering opportunities to study the evolution of numerous lineages within the superfamily. Based on published records and our direct examination of specimens, the platygastroid fauna in Eocene amber is a combination of extant and extinct genera (Johnson et al. 2008). This contrasts with the fauna in Dominican amber, which is equivalent to the extant fauna at the generic level (Talamas and Buffington 2015), and Cretaceous amber, for which all genera but one, *Archaeoteleia* Masner, are extinct (excluding misplaced species) (Johnson et al. 2008; Ortega-Blanco et al. 2014; Talamas et al. 2017; Talamas et al. 2019). The intermediate age of Eocene fossils thus requires intimate experience with

the preceding and subsequent faunas to appropriately place species and infer phylogenetic relationships.

We here describe a new species from Baltic amber in the extant genus *Janzenella* Masner & Johnson. *Janzenella* has a distinct metasoma in which the anterior margins of the first tergite and sternite are non-carinate, a form found only in *Janzenella* and the scelionid genus *Mantibaria* Kirby (Masner and Johnson 2007). In conjunction with other diagnostic characters, this enabled us to place the species in *Janzenella*, but we were unwilling to describe it as new because many important characters were occluded by the amber matrix. This obstacle has been overcome using a synchrotron and 3D reconstruction software, enabling us to visualize external morphology for species description as well as internal characters of phylogenetic significance.

Material and methods

Photographs were taken with a Leica DMRB compound microscope with a GT-Vision Lw11057C-SCI digital camera attached and rendered using the program CombineZP, or with a Macropod Microkit with images rendered using Helicon Focus. Some specimens for electron microscopy were coated in ~70 nm of gold/palladium using a Cressington sputter coater and imaged with a Hitachi TM3000 Tabletop Microscope at 15 keV. Uncoated specimens were imaged using a Phenom XL G2 Desktop SEM at 5 keV. In some cases, multiple images were stitched in Adobe Photoshop to provide larger images with high resolution and magnification.

Synchrotron microtomography was performed at the imaging cluster of the KIT light source of Karlsruhe Institute of Technology using a parallel polychromatic X-ray beam produced by a 1.5 T bending magnet. Scans were done by taking 3,000 projections at 70 frames per second and an optical magnification of 10×, resulting in an effective pixel size of 1.22 µm. The beam was spectrally filtered by 0.2 mm aluminum with a spectrum peak at about 15 keV and a full-width at half maximum bandwidth of about 10 keV. A fast indirect detector system was employed, consisting of a 10 µm (10×) LuAG:Ce scintillator, diffraction limited optical microscope (Optique Peter) and a 12bit pco.dimax high speed camera with 2016 × 2016 pixels. We used the control system concert (Vogelgesang et al. 2016) for automated data acquisition and online reconstruction of tomographic slices for data quality assurance. Online data processing was performed by the UFO framework (Vogelgesang et al. 2012). The resulting cross-sections were rendered into 3D models and manipulated using the 3D Viewer and Volume Viewer plugins in ImageJ (FIJI) (Schmid et al. 2010; Schindelin et al. 2012; Rueden et al. 2017). Models were further refined to improve character resolution with 3DSlicer 4.11 (Fedorov et al. 2012).

The raw scan images are available individually at https://doi.org/10.5281/zenodo.4608043, and as a multipage tiff at https://doi.org/10.5281/zenodo.4608412. All rendered images, including those not included as figures are available at https://doi.org/10.5281/zenodo.4608788.

Character annotations

amem anterior extension of the mesofurca (Figure 14)
fu1a profurcal arms (Figure 13)
fu2 mesofurca (Figure 14)
fu3 metafurca (Figure 15)
lmfa lateral mesofurcal arms (Figure 14)
lo lateral ocellus (highlighted in red) (Figure 8)
mo median ocellus (Figure 8)
mnt metanotum (Figures 11, 12)
ts tibial spur (Figures 16, 17)

Taxonomy

Janzenella Masner & Johnson

Janzenella Masner & Johnson, 2007: 2 (original description. Type: *Janzenella innupta* Masner & Johnson, by monotypy and original designation).

Note. Our generic description comprises the characters shared by *J. innupa* and *J. theia*, and thus is largely a reduction of the description of *J. innupta* provided by Masner & Johnson (2007). Two characters, the tibial spur formula and the morphology of internal apodemes, were not assessed for both species but are assumed to be stable within the genus. Nomenclature of internal structures follows Mikó et al. (2007).

Description. Small, elongate, length 1.2–1.3 mm; body strongly depressed, with relatively short legs and antennae; macropterous.

Head. Head transverse in dorsal view, width 1.5 times length, somewhat narrowed medially; hyperoccipital carina absent, head in frontal view wider than high, height 0.8 times width; frons largely flat to weakly convex, smooth; interantennal process absent, torulus large, opening forward, lower rim of torulus nearly reaching oral cavity; submedian carina absent; orbital carina absent, lower frons reflexed ventrally; inner orbits rounded, diverging dorsally and ventrally; clypeus very small, triangular, not differentiated into postclypeus, anteclypeus; malar sulcus absent; malar and facial striae absent; labrum not visible externally; mandible short, robust, tridentate, teeth subequal in size; antenna 11-merous; radicle inserted apically into A1, nearly parallel to axis of A1; A1 short, strongly widened in apical half, apex excavate for reception of flagellum; A3 distinctly shorter than A2; A3–A5 globular; apical 4 antennomeres expanded into semiabrupt clava in female; papillary sensilla on female antenna arranged in longitudinal pairs on apical antennomeres; claval formula A8–A11: 2-2-2-1.

Mesosoma. Mesosoma strongly depressed, in dorsal view longer than wide, in lateral view distinctly longer than high; pronotum in dorsal view narrowed laterally; subparallel to outline of mesoscutum, anterolateral corners rounded, anterior

face extended forward into necklike elongation; transverse pronotal carina absent; vertical epomial carina absent; horizontal epomial carina present; lateral face of pronotum largely flat to weakly concave, without scrobe for reception of foreleg, anterior margin very finely foveolate; netrion absent; anterior margin of mesoscutum meeting pronotum dorsally; admedian lines absent; parapsidal lines absent, notauli absent; skaphion absent; mesoscutum with roughly circular punctate areas present on either side; transscutal articulation well developed, simple; scutellum wider than long, unarmed, nearly flat; metanotum extremely narrow, striplike, dorsellum not differentiated, keels, plicae of propodeum not developed; mesopleural carina absent; acetabular carina fine, anterior margin of ventral portion of mesepisternum straight, not projecting between fore coxae; posterior margin of mesopleuron with complete line of foveolae extending from base of forewing to mid coxa; episternal foveae absent; anteroventral portion of metapleuron rounded, not separated from lateral face by carina, metapleural pit not apparent; posterior margin of metapleuron rounded; metapleuron above hind coxa reticulate, otherwise smooth; lateral propodeum without longitudinal carinae, posterolateral corner not produced posteriorly, posterior margin broadly rounded; legs relatively short, slender, only hind femur somewhat enlarged; tarsal formula 5-5-5; forewing extending to apex of metasoma, R bifurcating apically, bulla absent; R1 absent or extremely short, therefore without postmarginal vein; r-rs (stigmal vein) present, at least longer than R1; hindwing with R very short; tibial spur formula: 1-2-2.

Metasoma. Metasoma weakly sclerotized, loosely articulated, depressed; T1–T3 subequal in length; 7 terga, 6 sterna visible externally; laterotergites extremely wide, no submarginal ridge present; laterosternites absent; no spiracles visible; anterior margin of segment 1 without anterior carina, T1 and S1 rounded and prolonged anteriorly into short neck that inserts into propodeal foramen; sutures between all segments simple, terga and sterna broadly overlapping; anterior margin of S2 straight; narrow sublateral felt fields absent.

Internal morphology. Profurca without dorsal bridge, anterior profurcal lamellae forming long, slender processes that extend anteriorly over the basisternum; mesofurca Y-shaped, lacking an apparent dorsal bridge; metafurca slanted anteriorly, metafurcal arms simple, straight, rod-like.

Janzenella theia Bremer & Talamas, sp. nov.

http://zoobank.org/3429DDD3-FDC4-40E7-84AB-3E18EBF8C057

Description. Width of head decreasing anteriorly, occiput in dorsal view strongly excavated, lateral ocellus separated from inner orbit by approximately one ocellar diameter, compound eye relatively large, its length approximately 0.75 that of the head in lateral view; interorbital space broad, approximately equal to height of compound eye; mesoscutum 1.3 times wider than long; femoral depression shallow, weakly defined; forewing with R straight basally, curving toward anterior margin in distal third, R sepa-

Figures 1, 2. *Janzenella theia* (USNMENT01223652), head, mesosoma, metasoma, brightfield photography **1** dorsolateral view **2** ventrolateral view.

rated from costal margin by at least the width of the vein, r-rs (stigmal vein) straight, much longer than wide (>3×); 1Rs, 1Rs+1M, 2Rs, M, and Cu present as spectral veins; propodeum with coarse rugae radiating from propodeal foramen.

Material examined. Holotype female, USNMENT01223652 (Hoffeins #0002-7), Kaliningrad, Russia, coll. Yantarny, 2015 (deposited in Senckenberg Deutsches Entomologisches Institut, Müncheberg, Germany).

Diagnosis. *Janzenella theia* differs from *J. innupta* in just a few notable characters. The compound eyes of *J. theia* are significantly larger than those of *J. innupta*, occupying most of the lateral head (compare Figures 5, 6). *Janzenella theia* also lacks the

Figures 3, 4. *Janzenella theia* (USNMENT01223652), head, mesosoma, metasoma **3** lateral view **4** anterolateral view.

pronounced genal swelling that gives the head a quadrate appearance in *J. innupta*. In the forewing of *J. theia*, R is separated from the wing margin by at least the width of the vein, and r-rs is much longer than wide (>3×) (Figures 2, 10), contrasting that of *J. innupta* in which R reaches the costal margin and the length of r-rs is about equal to its width (Figure 9). The propodeum of *J. theia* has coarse rugae radiating from the propodeal foramen (Figure 12) whereas *J. innupta* has rugose-areolate sculpture with submedian smooth patches (Figure 11).

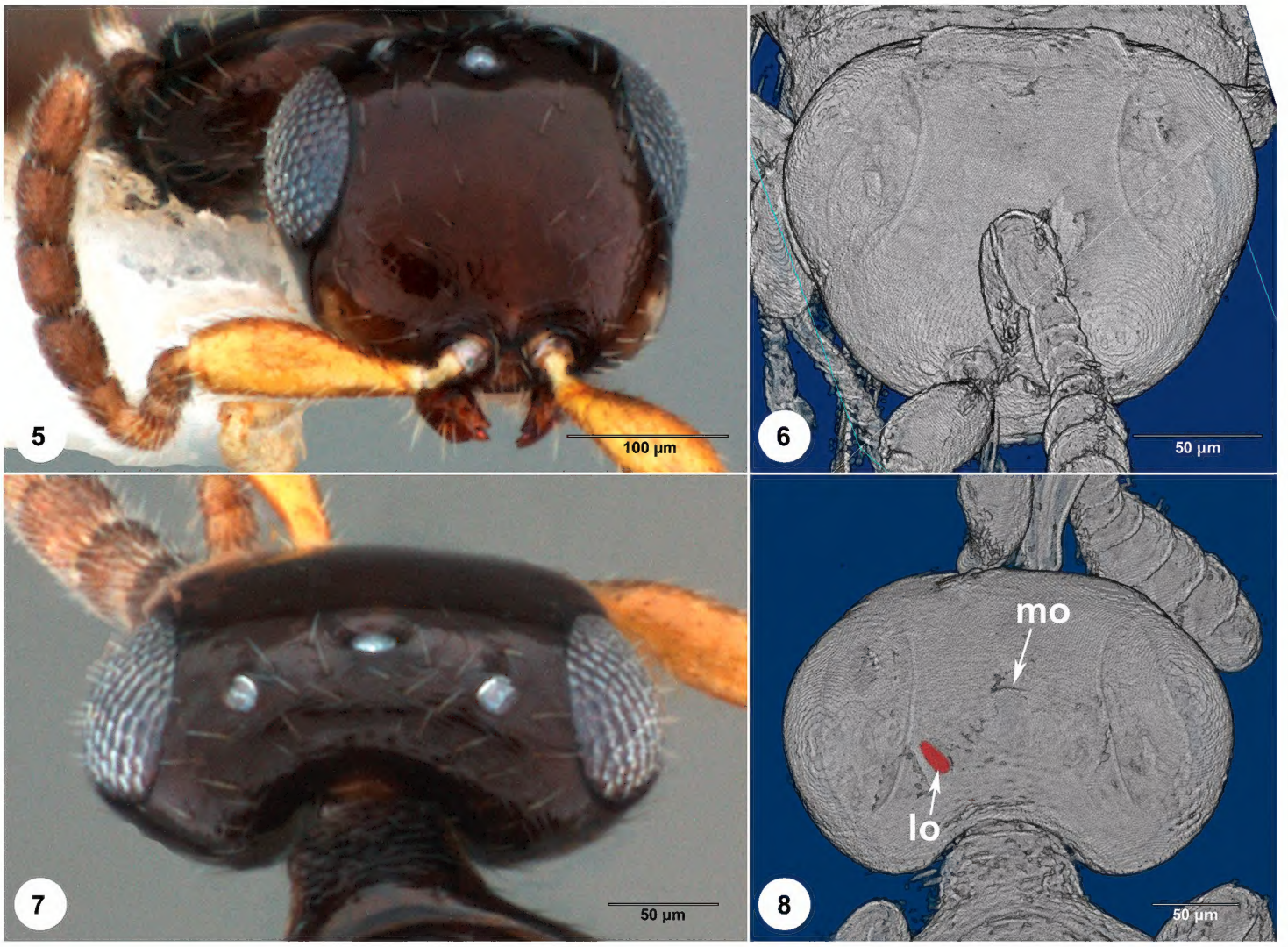

Figures 5–8. **5** *Janzenella innupta* (OSUC 264384), head, anterior view **6** *J. theia* (USNMENT01223652), head, anterior view **7** *J. innupta* (OSUC 264384), head, dorsal view **8** *J. theia* (USNMENT01223652), head, dorsal view.

Etymology. The species is named after Theia, the mythical Greek titaness of sight, who is credited with endowing precious stones with their brilliance and intrinsic value. The name is treated as an appositional noun.

Discussion. *Janzenella theia* and *J. innupta* are remarkably similar (compare Figures 1–4 to 18, 19) given the span of time between the Eocene and the present, as is evidenced by the brevity of our species description and length of the generic description. This similarity, and the conspecificity of *J. innupta* specimens in Dominican amber and from Costa Rica (Masner and Johnson 2007), support the notion that morphological change occurs very slowly in *Janzenella*. We included two characters in our generic description that were assessed in only one of the species. The tibial spurs in *Janzenella innupta* are very small and required use of high magnification microscopy to confidently assess their number (Figures 16, 17), we were not able to determine their number on *J. theia*, but given that a 1-2-2 tibial spur formula is plesiomorphic for the superfamily (Chen et al. 2021), we consider it reasonable to believe that the older species has the same configuration. The pro-, meso- and metafurcae are clearly visible in the reconstructions of *J. theia* (Figures 13, 14) but we have not yet examined these structures in *J. innupta*. Given the similarity of *J. theia* and *J. innupta*, we treat these characters as stable within *Janzenella* for the purposes of comparative analysis.

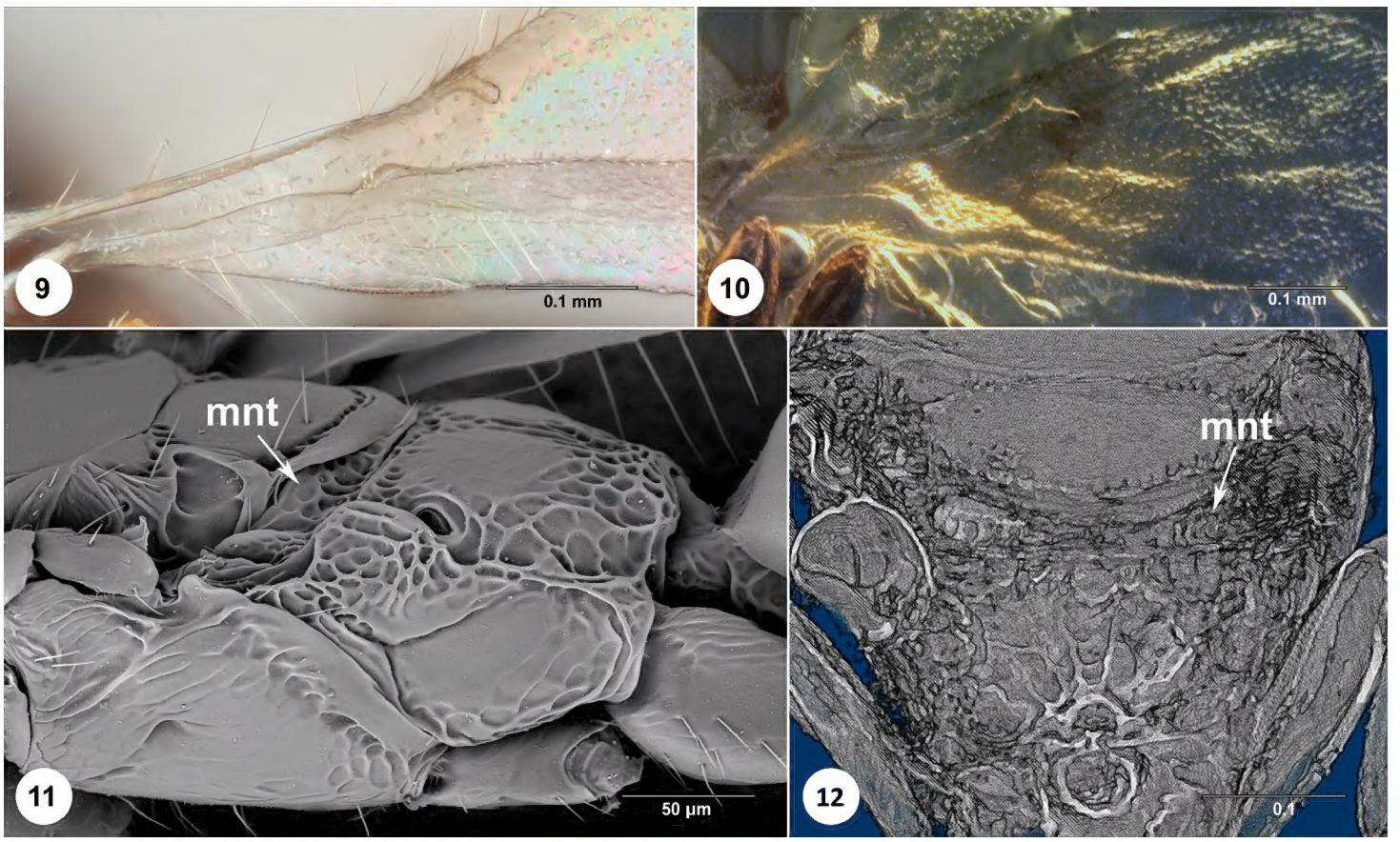

Figures 9–12. 9 *Janzenella innupta* (OSUC 264400), fore and hind wings, dorsal view **10** *J. theia* (USNMENT01223652), fore and hind wings, ventral view **11** *J. innupta* (OSUC 264384), mesosoma, dorsolateral view **12** *J. theia* (USNMENT01223652), mesosoma, posterodorsal view.

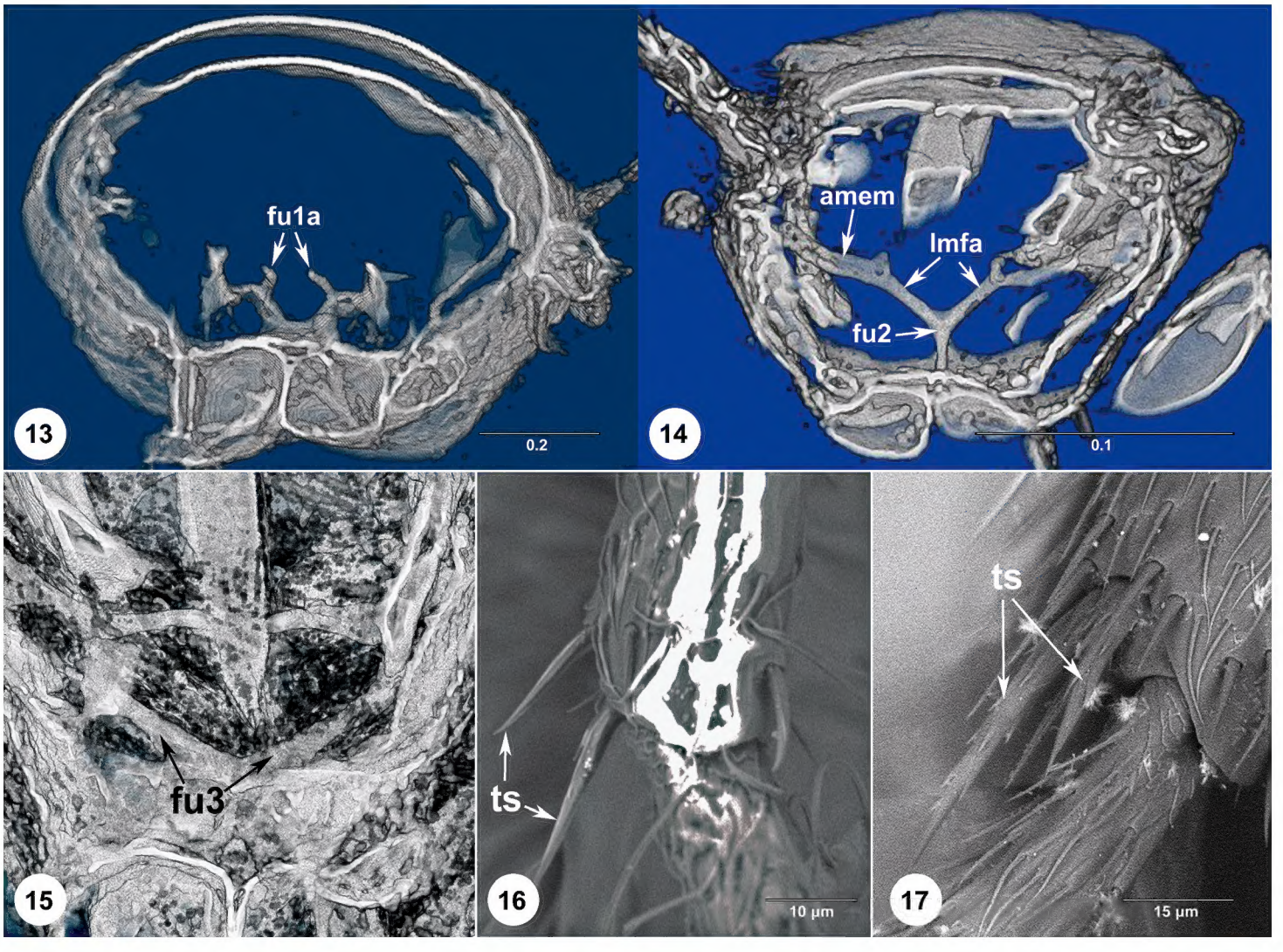

Figures 13–17. 13 *Janzenella theia* (USNMENT01223652), profurca, posterior view **14** *J. theia* (USNMENT01223652), mesofurca, posterior view **15** *J. theia*, metafurca, posterior view **16** *J. innupta* (OSUC 264397), mesotibia, lateral view **17** *J. innupta* (OSUC 264397), metatibia, lateral view.

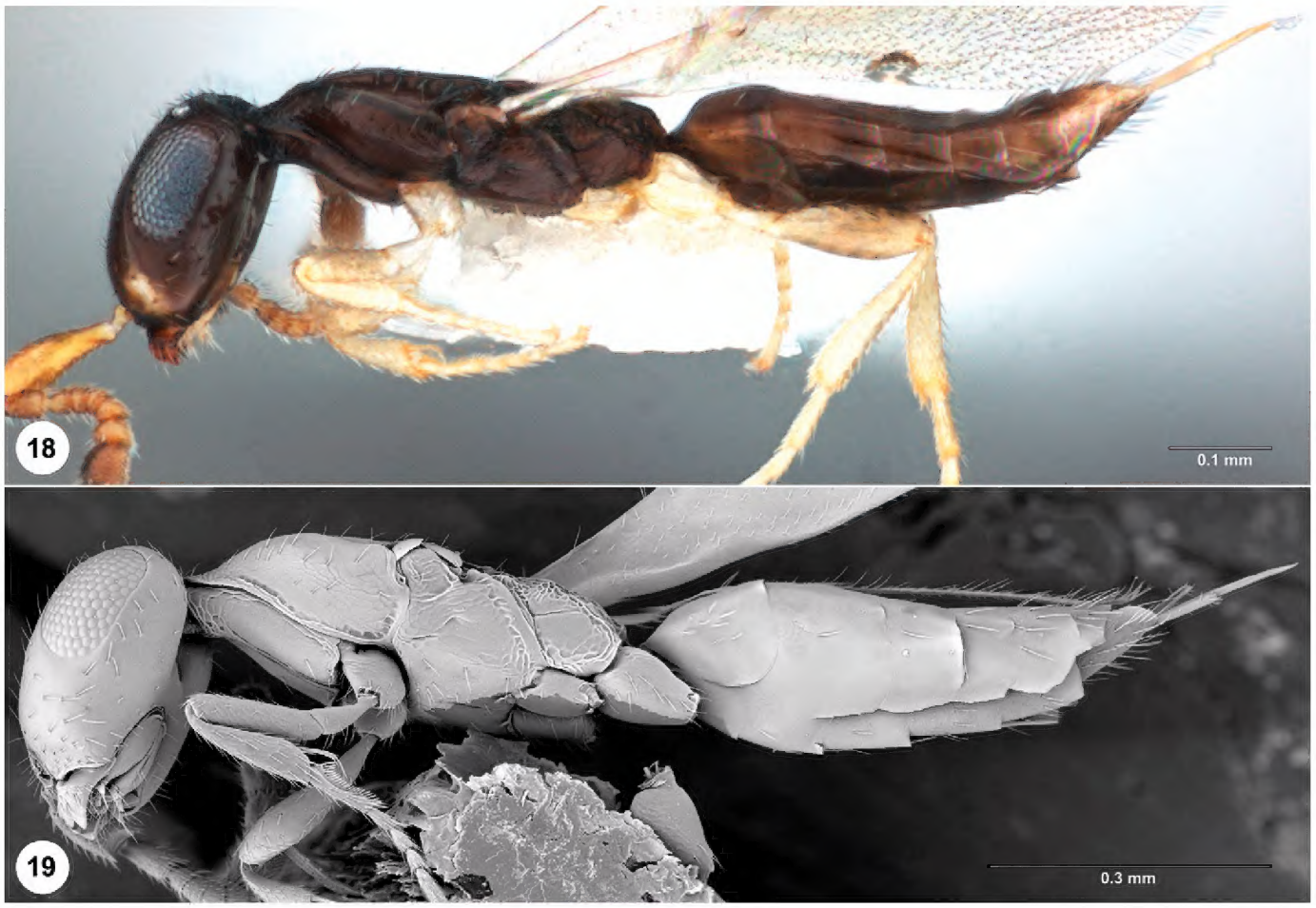

Figures 18, 19. *Janzenella innupta* (OSUC 264384), head, mesosoma, metasoma, lateral view.

Metanotum. The lateral metanotum in *J. innupta* (Figure 11) is rugose in addition to the line of foveae along the posterior part of the sclerite. Such sculpture on this part of the metanotum (metanotal trough in taxa where the metascutellum is visible) is otherwise unknown to us in Platygastroidea. We were not able to resolve this detail in the rendered images of *J. theia*.

Profurca. Vilhelmsen et al. (2010) found the profurcal bridge to be absent in Platygastroidea, although it has since been found to exist in the platygastrid genus *Amitus* Haldeman (Mikó et al. 2021). The absence of the profurcal bridge in *Janzenella* is congruent with treating this as a plesiomorphic condition, although internal characters have yet to be examined in the recently erected families Geoscelionidae, Proteroscelionidae, and Neuroscelionidae (Talamas et al. 2019; Chen et al. 2021).

Mesofurca. Mikó et al. (2007) reported the presence of a mesofurcal bridge in Scelionidae, which at that time contained lineages now treated as Nixoniidae and Sparasionidae (Chen et al. 2021). Mikó et al. (2021) reported two forms in Platygastridae: without a bridge in *Amitus* and with a bridge in *Synopeas* Förster. Heraty et al. (1994) determined the mesofurcal bridge to be absent in Platygastridae based on examination of two genera (*Isocybus* Förster and *Inostemma* Haliday) and considered that these losses were apomorphies. The absence of a mesofurcal bridge in *J. theia* thus may indicate close relation to Platygastridae, as was suggested by the analyses of Chen et al. (2021). However, the presence of a mesofurcal bridge in *Synopeas* reflects the need for greater taxon sampling in Platygastridae to confidently establish the plesiomorphic condition for Platygastridae and to determine if loss of the mesofurcal bridge is indeed irreversible as Heraty et al. (1994) suggested.

Conclusion

The phylogenetic treatment of Chen et al. (2021) elevated *Janzenella* into a family, which was retrieved in a trichotomy with Platygastridae and Neuroscelionidae. Given that Platygastridae is found in Burmese amber and clearly recognizable at the family level (Talamas et al. 2019, Talamas et al. 2021), we speculate that Janzenellidae might also be easily recognized if encountered in Cretaceous amber. At present, we are analyzing an undescribed taxon from Burmese amber with a metasoma much like that of *Janzenella*. This comparative analysis has just begun, but already foretells more exciting discoveries in the evolution of Platygastroidea.

Acknowledgments

We thank Christel Hoffeins, whose loan of Baltic amber made this study possible, and Dr. Lubomír Masner, Canadian National Collection of Insects, who kindly provided specimens of *J. innupta* for comparative analysis. Jonathan Bremer and Elijah Talamas were supported by the Florida Department of Agriculture and Consumer Services- Division of Plant Industry.

References

Chen H-y, Lahey Z, Talamas EJ, Valerio AA, Popovici OA, Musetti L, Klompen H, Plaszek A, Masner L, Austin AD, Johnson NF (2021) An integrated phylogenetic reassessment of the parasitoid superfamily Platygastroidea (Hymenoptera: Proctotrupomorpha) results in a revised familial classification. Systematic Entomology 46(4): 1088–1113. https://doi.org/10.1111/syen.12511

Fedorov A, Beichel R, Kalpathy-Cramer J, Finet J, Fillion-Robin J-C, Pujol S, Bauer C, Jennings D, Fennessy FM, Sonka M, Buatti J, Aylward SR, Miller JV, Pieper S, Kikinis R (2012) 3D Slicer as an Image Computing Platform for the Quantitative Imaging Network. Magn Reson Imaging. 30: 1323–1341. https://doi.org/10.1016/j.mri.2012.05.001

Heraty JM, Woolley JB, Darling DC (1994) Phylogenetic implications of the mesofurca and mesopostnotum in Hymenoptera. Journal of Hymenoptera Research 3: 241–277.

Johnson NF, Masner L, Musetti L (2008) The Cretaceous scelionid genus *Proteroscelio* Brues (Hymenoptera: Platygastroidea). American Museum Novitates 3603: 12–17. https://doi.org/10.1206/0003-0082(2008)3603[1:TCSGPB]2.0.CO;2

Masner L, Johnson NF (2007) *Janzenella*, an Enigmatic New Genus of Scelionid Wasp from Costa Rica (Hymenoptera: Platygastroidea, Scelionidae). American Museum Novitates 3574: 1–7. https://doi.org/10.1206/0003-0082(2007)3574[1:JAENGO]2.0.CO;2

Mikó I, Raymond M, Talamas EJ (2021) New family-level characters for Platygastroidea. In: Lahey Z, Talamas E (Eds) Advances in the Systematics of Platygastroidea III. Journal of Hymenoptera Research 87: 235–249. https://doi.org/10.3897/jhr.87.72906

Mikó I, Vilhelmsen L, Johnson NF, Masner L, Pénzes Z (2007) Skeletomusculature of Scelionidae (Hymenoptera: Platygastroidea): head and mesosoma. Zootaxa 1571: 1–78. https://doi.org/10.11646/zootaxa.1571.1.1

Ortega-Blanco J, McKellar RC, Engel MS (2014) Diverse scelionid wasps in Early Cretaceous amber from Spain (Hymenoptera: Platygastroidea). Bulletin of Geosciences 89: 553–571. https://doi.org/10.3140/bull.geosci.1463

Rueden CT, Schindelin J, Hiner MC, DeZonia BE, Walter AE, Arena ET, Eliceiri KW (2017) ImageJ2: ImageJ for the next generation of scientific image data. BMC Bioinformatics 18: e529. https://doi.org/10.1186/s12859-017-1934-z

Schindelin J, Arganda-Carreras I, Frise E, Kaynig V, Longair M, Pietzsch T, Preibisch S, Rueden C, Saalfeld S, Schmid B, Tinevez J-Y, White DJ, Hartenstein V, Eliceiri K, Tomancak P, Cardona A (2012) Fiji: an open-source platform for biological-image analysis. Nature methods 9: 676–682. https://doi.org/10.1038/nmeth.2019

Schmid B, Schindelin J, Cardona A, Longair M, Heisenberg (2010) A high-level 3D visualization API for Java and ImageJ. BMC Bioinformatics 11: 1–1. https://doi.org/10.1186/1471-2105-11-274

Talamas EJ, Johnson NF, Shih C, Ren D (2019) Proterosceliopsidae: A new family of Platygastroidea from Cretaceous amber. In: Talamas E (Eds) Advances in the Systematics of Platygastroidea II. Journal of Hymenoptera Research 73: 3–38. https://doi.org/10.3897/jhr.73.32256

Talamas EJ, Buffington ML (2015) Fossil Platygastroidea in the National Museum of Natural History, Smithsonian Institution. Journal of Hymenoptera Research 47: 1–52. https://doi.org/10.3897/JHR.47.5730

Talamas EJ, Johnson NF, Buffington ML, Dong R (2016) *Archaeoteleia* Masner in the Cretaceous and a new species of *Proteroscelio* Brues (Hymenoptera, Platygastroidea). In: Talamas EJ, Buffington ML (Eds) Advances in the Systematics of Platygastroidea. Journal of Hymenoptera Research 56: 241–261. https://doi.org/10.3897/jhr.56.10388

Talamas EJ, Popovici O, Shih C, Ren D (2021) *Prototeleia* Talamas, Popovici, Shih & Ren: A new genus of Platygastridae from Burmese amber. In: Lahey Z, Talamas E (Eds) Advances in the Systematics of Platygastroidea III. Journal of Hymenoptera Research 87: 67–80. https://doi.org/10.3897/jhr.87.65472

Vilhelmsen L, Mikó I, Krogmann L (2010) Beyond the wasp-waist: structural diversity and phylogenetic significance of the mesosoma in apocritan wasps (Insecta: Hymenoptera). Zoological Journal of the Linnaen Society 159: 22–194. https://doi.org/10.1111/j.1096-3642.2009.00576.x

Vogelgesang M, Chilingaryan S, dos Santos Rolo T, Kopmann A (2012) UFO: A scalable GPU-based image processing framework for on-line monitoring." 2012 IEEE 14th International Conference on High Performance Computing and Communication & 2012 IEEE 9th International Conference on Embedded Software and Systems, 824–829. https://doi.org/10.1109/HPCC.2012.116

Vogelgesang M, Farago T, Morgeneyer TF, Helgen L, dos Santos Rolo T, Myagotin A, Baumbach T (2016) Real-time image-content-based beamline control for smart 4D X-ray imaging. Journal of synchrotron radiation 23.5: 1254–1263. https://doi.org/10.1107/S1600577516010195